Control of Superselectivity by Crowding in Three-Dimensional Hosts

Andrew T. R. Christy,[1] Halim Kusumaatmaja,[2,*] and Mark A. Miller[1,†]
[1]Department of Chemistry, Durham University, South Road, Durham DH1 3LE, United Kingdom
[2]Department of Physics, Durham University, South Road, Durham DH1 3LE, United Kingdom

(Received 6 June 2020; accepted 9 December 2020; published 11 January 2021)

Motivated by the fine compositional control observed in membraneless droplet organelles in cells, we investigate how a sharp binding-unbinding transition can occur between multivalent client molecules and receptors embedded in a porous three-dimensional structure. In contrast to similar superselective binding previously observed at surfaces, we have identified that a key effect in a three-dimensional environment is that the presence of inert crowding agents can significantly enhance or even introduce superselectivity. In essence, molecular crowding initially suppresses binding via an entropic penalty, but the clients can then more easily form many bonds simultaneously. We demonstrate the robustness of the superselective behavior with respect to client valency, linker length, and binding interactions in Monte Carlo simulations of an archetypal lattice polymer model.

DOI: 10.1103/PhysRevLett.126.028002

Superselectivity is the sensitive response of binding to the density of binding receptors. If a system exhibits superselectivity then there is a characteristic receptor density at which the binding species changes sharply from being mostly free to mostly bound [1]. This effect is desirable whenever a clean switch is required in response to a well-defined trigger. Applications include tumor treatment (where target cells can be recognized by the anomalous expression of certain receptors on their surface) [2], targeted drug delivery [3], and self-assembly in material chemistry [4]. Superselectivity is also exploited by nature in cell signaling and immunology [5] because the steplike transition allows binding to be finely controlled [6]. Superselectivity relies on the binding species being multivalent; it is the ability of multivalent particles to form many combinations of multiple, weak connections that makes the binding sensitive to receptor concentration while still providing a strong overall interaction [1,7].

The archetypal model of superselective binding is a surface decorated with binding receptors and a nanoparticle coated with ligands. Binding is triggered when the surface density of receptors is high enough for the nanoparticle to interact with many receptors simultaneously [1]. A similar effect at a surface can be achieved when the binding species is a multivalent polymer, where multiple binding sites along the polymer play the role of the ligands grafted onto the nanoparticle [6].

In contrast to existing work on superselective binding at surfaces, here we examine whether superselectivity can also be observed for receptors embedded in a porous three-dimensional (3D) structure. Significant motivation for this work comes from membraneless droplet organelles. These cellular substructures are formed by mechanisms resembling liquid-liquid phase separation (LLPS) [8]. Their functions range from providing spatiotemporal organization of cellular materials to tuning biochemical reactions inside cells [9] and improving cellular fitness during stress [10,11]. To achieve these functions, membraneless organelles exhibit finely tuned compositional control but the mechanisms of their operation are incompletely understood.

The interaction of molecules with droplet organelles has recently been described in terms of a client-scaffold model [12], where the scaffold is a relatively stable structure arising from the LLPS process and consists of several protein and RNA species. The clients are other molecular species that can be expelled from or recruited into the droplet comparatively quickly in response to changes in the cellular environment. A client may be located transiently in the droplet while the droplet scaffold is effectively static.

Here, we use coarse-grained simulations of the client-scaffold model to demonstrate that superselectivity provides a plausible mechanism for compositional control in droplet organelles: small variations in the cellular environment can shift the system across the superselective transition, thus determining whether a species is found within or outside a droplet organelle. Moving from a surface to a 3D binding scaffold, we demonstrate how crowding species can be exploited to manipulate superselective binding. Membraneless organelles often contain numerous protein types and RNA species [13], which can act as crowders within the scaffold. To the best of our knowledge, this role of molecular crowding in superselective binding has not been identified before. We rationalize the behavior using entropic arguments, systematically evidenced by varying the key parameters. We also show that the superselectivity effect is not reliant on details of the client-receptor interaction model.

 © 2021 American Physical Society

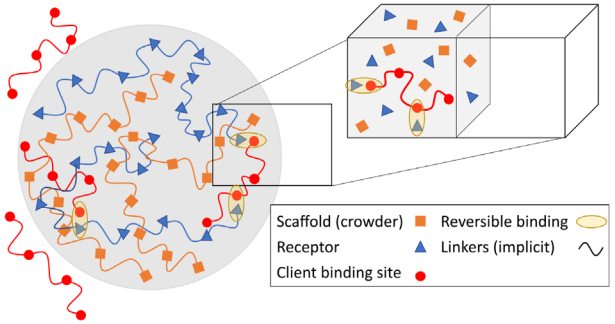

FIG. 1. Schematic of the simulation setup. Three types of molecules are simulated, corresponding to client, receptor, and crowder beads. The beads are connected by flexible implicit linkers.

Our computational model is illustrated schematically in Fig. 1. There are three types of particle, which all occupy vertices on a cubic lattice. The receptor sites of the scaffold (blue triangles) can reversibly form bonds with the binding sites on the client molecule (red circles) if they lie on adjacent sites. In addition, the scaffold has crowder beads (orange squares) that occupy a lattice site but have no energetic interactions with other particles. A lattice site may host at most one bead, giving all the beads equal excluded volume. In this work, the scaffold is represented by a random distribution of individual receptor and crowder beads for generality. This approach gives equivalent results to a scaffold of cross-linked polymers for the same receptor and crowder densities, but avoids the results depending on arbitrary details of the scaffold's initialization. The client is a chain of binding sites connected by flexible "implicit" linkers, as introduced in the Flory random coil model of Harmon *et al.* [14]. The linkers have a specified maximum length (in lattice units), limiting the separation of connected client beads, but the linkers are not represented explicitly and are treated as occupying negligible volume.

The simulations are performed on a lattice of $50 \times 50 \times L$ sites with periodic boundary conditions in all directions. Except where specified, $L = 100$. Scaffold beads (receptors and crowders) are confined to a slab of thickness 50 sites in the long direction of the cell and periodic in the other two dimensions. The scaffold-free region of length $L - 50$ lattice sites adjoining the slab represents the cytosol. In the client-scaffold model, the client is treated as being far more mobile than the scaffold structure. Thus, the client explores the system while the scaffold remains fixed. The immobilization of the scaffold is justified by experimental evidence showing a large variation in retention times of species within membraneless organelles [15–17], with client molecules having significantly higher diffusion rates than scaffold components [18]. Furthermore, in line with previous work on client-scaffold systems [12,19], we focus on the dilute regime, where the client concentration is low compared to the scaffold. For simplicity, we work with a single client but, as shown in the Supplemental Material [20], explicit simulation of multiple clients leads to the same results per client. To ensure statistically significant results, all measurements are averaged over runs with multiple (typically 40) independent scaffold configurations.

The components of membraneless organelles include multivalent species with well defined binding regions that can accept one ligand each [25], as well as intrinsically disordered proteins or regions of proteins with less specific attraction [26]. To mimic these, we consider both specific directional and isotropic interactions between the receptor and client beads [27]. For isotropic interactions, all client beads adjacent to receptor beads are bound, while for specific directional interaction, the receptor bead can form at most one bond. A directional bond must be broken for either bead to form a new bond. We define the bonding interaction energy $-f$ (with $f > 0$ for attractive interactions) with reference to the temperature, making f/kT the relevant control parameter. Configuration space is sampled canonically by Monte Carlo steps that alter the client conformation and bonding arrangements; details of the algorithms are provided in the Supplemental Material [20]. For each scaffold snapshot, the typical number of Monte Carlo sweeps for the client is 10^8.

We define a probability θ of the client being bound by at least one bead to the scaffold at a given receptor density n_R (fraction of lattice sites occupied by receptors). In our dilute 3D system, this probability is analogous to the fraction of bound particles in studies of binding at two-dimensional substrates [1,6,28]. Figure 2(a) shows the binding probability as a function of receptor density for decavalent clients in both the isotropic and directional binding cases and in systems with and without crowders. The volume ratio between the scaffold and free regions is 1. For reference, we also include corresponding results for a single monovalent client. The transition from unbound to bound is sharper and occurs within a narrower range of receptor densities for the decavalent client when crowders are

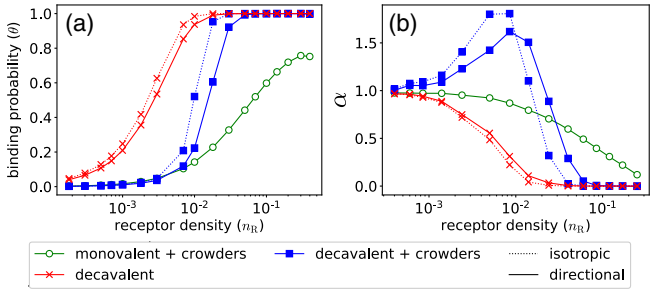

FIG. 2. Client binding in the isotropic and directional binding models. The density of crowders (where present) is 0.4. (a) Binding probability θ as a function receptor density n_R. (b) Superselectivity parameter α as a function of receptor density. The interaction strength between receptors and binding beads is $f = 2kT$ and linkers connecting the binding beads have a length of 5 lattice spacings.

present. Furthermore, the sharpness of the increase relative to that of the monovalent client resembles the superselective behavior observed in surface binding [28].

To quantify the rate at which binding responds to receptor density, we use the parameter

$$\alpha = \frac{d \ln \theta}{d \ln n_R}, \tag{1}$$

as introduced by Martinez-Veracoechea and Frenkel [1] for nanoparticles binding at a surface. Here, however, we emphasize that n_R is the density (concentration) of receptors in three dimensions. By construction, α falls monotonically from 1 to 0 with increasing receptor density for any client whose free energy of binding is independent of that density. This is the case for a one-bead monovalent client, as shown by the green circles in Fig. 2(b). In contrast, if the binding free energy is sufficiently sensitive to receptor density at low θ, then α may exhibit a peak above 1, indicating a sharp response of binding to receptor density and the presence of superselectivity.

For binding at a surface, superselectivity is readily achieved when the binding species is multivalent. However, in a 3D scaffold containing only binding sites, this is not always the case. When the volumes of the scaffold and free regions are comparable, we do not observe superselectivity for any combination of client valency, linker length, or binding strength; the red lines for a decavalent client in Fig. 2(b) are typical, with α never exceeding 1. Nevertheless, superselectivity can be achieved for both the isotropic and the directional bonding cases by the introduction of inert crowders, as shown by the peaks at $\alpha > 1$ of the blue lines in Fig. 2(b).

As in the surface-binding case, superselectivity in 3D has an entropic origin: binding is initially suppressed due to an entropic penalty, but the client can then more easily form many bonds simultaneously [29]. At a surface, the initial decrease in entropy on binding of a flexible polymeric client arises from both the loss of translational freedom and the restriction on internal conformations imposed by the surface. Figure 2(b) shows that, in a sparse 3D scaffold, the loss of translational entropy alone may not be sufficient to cause superselectivity, and the conformational entropy must be further controlled by crowding to achieve it.

To quantify this argument, we measure the distribution of the number of bonds that the decavalent client (with directional binding) forms with the receptors. The resulting histograms are shown in Fig. 3. For reference, we have also shown the probability that m of ten independent monomers are bound in the dilute limit, derived from simulations of a single monomer and binomial statistics.

The results without crowders are shown in Fig. 3(a). For clarity, we show the probabilities only for $m = 0$, 1, 5 and 9 bound beads. The probabilities for $m = 0$, 1, and 5 are very similar for the multivalent client and the ten independent monomers, showing there is little cooperative binding effect. An increase in the multivalent probability is only observed for $m = 9$ at a density regime where the chain is already fully bound and superselectivity is not affected.

The case with crowders is shown in Fig. 3(b). In contrast to panel (a), we see an anticooperative binding effect for small m, relevant at low receptor density where binding is significantly suppressed for the decavalent client compared to independent monomers. This is followed by a similar binding probability for intermediate m, and then a cooperative effect enhancing the binding probability for larger m at higher receptor density. This compression of the binding response into a narrower range of receptor density is the signature of superselectivity.

Figure 3(c) provides further insight into the thermodynamic origins of the superselectivity. The change in free energy compared to an unbound client (obtained from the

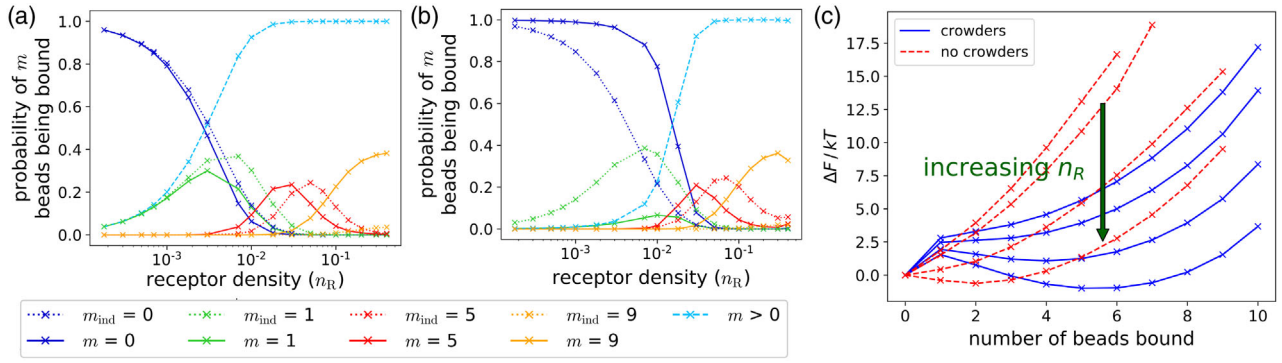

FIG. 3. Probability of m beads being bound in a decavalent client with linker length 5 (full lines), and the probability that m of 10 independent monomers (dotted lines) are bound in the directional binding model. (a) No crowders, (b) crowders at density 0.4. The $m > 0$ line shows the probability of the chain being bound (θ). (c) Change in free energy ($\Delta F/kT$) for the client to be bound by m beads in a system with and without crowders, with respect to an unbound client. The interaction energy between receptors and binding sites is $f = 2kT$.

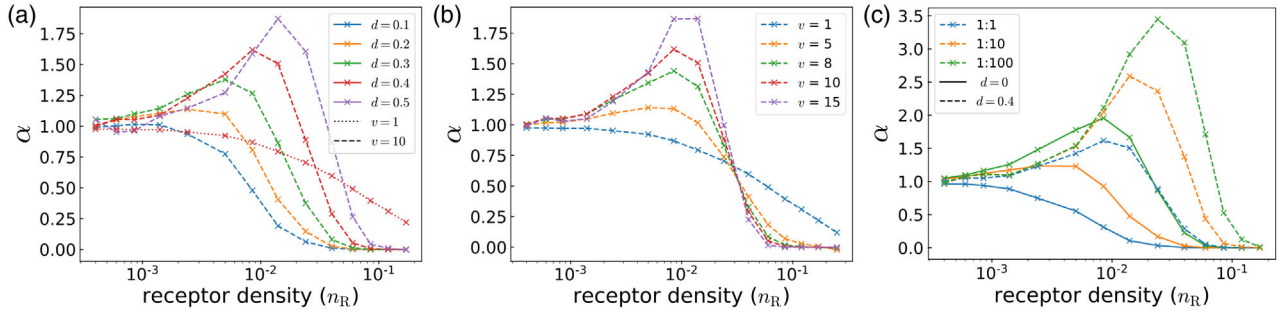

FIG. 4. Superselective parameter α as a function of receptor density for a range of client parameters in the directional binding model, varying (a) the density d of crowders in the scaffold, (b) the valency v of the client, and (c) the ratio of scaffold volume to free space. In (c), the results with ($d = 0.4$) and without ($d = 0.0$) crowders are compared.

logarithm of the probability distribution) is shown as a function of the number of bound beads in the decavalent client. A qualitative difference between the systems with and without crowders is observed. In both cases, the free energy develops a minimum at $m > 0$ as the receptor density increases. However, introducing crowders produces a barrier before the minimum and the location of the minimum is shifted to larger m. The barrier suppresses binding of the client to the receptors by a small number of bonds but, because the entropic penalty only has to be paid once, there is a rapid increase in the number of bound beads once the barrier is overcome, as required for superselectivity.

With this understanding in mind, we turn to the question of how the system parameters affect the degree of superselectivity. In particular, we expect that superselectivity can be maximized by control of the entropy loss associated with the early stages of binding, thereby enhancing cooperative effects beyond that point. The results of this parameter study are shown in Fig. 4. Unless it is the parameter being varied, the ratio of scaffold to free volume is 1:1, the client is decavalent with linker length of 5 (lattice units) and the interaction strength is $f/kT = 2$ in a scaffold with crowders at density $d = 0.4$.

First, we vary the crowder density. Figure 4(a) shows that superselectivity arises and is progressively enhanced as the density of the crowder beads is increased. This parameter systematically controls the initial entropic penalty for binding by restricting the conformations available to the client, allowing superselectivity to be tuned. The limit of superselective enhancement comes when the crowder density is so high that the client cannot penetrate the scaffold and is primarily bound at the scaffold surface. Crowders can also occlude receptors by occupying adjacent sites, thereby reducing the effective binding capacity of the scaffold at a given receptor density.

Second, we vary the valency v of the client chain, which in our model is the number of linked binding sites. Figure 4(b) shows that superselectivity increases with valency. As we have seen, the client's overall binding free energy must depend sufficiently sensitively on receptor density at the early stages of binding in order to exhibit superselectivity. At one extreme in Fig. 4(b), the monomeric client has no internal structure to facilitate such a dependence and α shows a monotonic decrease. Increasing the number of beads in the chain provides the scope for greater entropy loss on entering the dense 3D scaffold while also increasing the enthalpy of the fully bound state for a given interaction strength f. Hence, increasing v both raises the initial entropic barrier and helps to repay the free energy enthalpically, promoting superselectivity.

Third, we study the impact of the free to scaffold volume ratio. Until now crowding has been necessary to produce any superselective binding. However, as shown in Fig. 4(c), superselectivity also arises at sufficiently large volume ratio in the absence of crowders. This is because the entropic penalty required for superselectivity can be introduced by amplifying the loss of translational freedom in the unbound state. Nonetheless, even in this case, crowders are important because they strongly enhance the degree of superselective binding, thereby sharpening the binding transition. Microscopy data of various membraneless organelles show that there is a large distribution in the size of droplets and the separation between them, with a typical free to scaffold volume ratio of $O(1000)$, e.g., see [30–32]. In the Supplemental Material [20], we provide a simple statistical mechanical model to extrapolate accurately from computed binding curves to arbitrarily large volumes without further computational expense.

The linker length l, interaction strength f/kT and the choice of directional or isotropic bonding affect the extent of superselectivity only weakly. These dependencies are presented and rationalized in the Supplemental Material [20] for completeness. Isotropic binding introduces a different class of multiply bound client-receptor configurations compared to the directional case. However, the fact that this does not have a strong effect on superselectivity provides valuable evidence that superselectivity does not rely on details of the bonding model.

In summary, we have demonstrated the importance of inert crowders in superselective binding of a multivalent chainlike client to a 3D host of binding. The crowders produce an entropic barrier for the client to enter the 3D

scaffold, suppressing binding at low receptor density. Once this barrier is overcome, cooperativity derived from multivalency leads to a sensitive response of binding to increases in the receptor density. This additional consideration is essential when attempting to generalize from the conventional case of superselectivity at a surface.

The phenomenon of superselectivity may help explain how membraneless organelles exert fine control over the macromolecules that they recruit and expel in the context of simple descriptions like the client-scaffold model [12]. The binding receptors in such organelles are held in place by a network of macromolecular backbones, which in themselves constitute part of the background crowder density. Membraneless organelles are known to be susceptible to alteration by changes in the cellular environment, such as *p*H, salt concentration, and glucose availability, or by post translational modifications [15]. These provide a mechanism by which the scaffold structure and/or the interaction strengths between sites in the membraneless organelle can be tuned, which in turn can lead to expulsion or recruitment of a biomolecular condensate component.

Superselective binding in 3D hosts could be exploited in other supramolecular multivalent structures, such as hydrogels (which have shown potential for tissue engineering [33]) and biosensors [34]. Given their polymeric nature, these may be suitable scaffolds to which clients could be attached. Furthermore, supramolecular nanoparticles have been proposed for use in drug delivery [35], and superselectivity may facilitate different mechanisms for deploying the payload.

Our model for superselectivity in 3D hosts has been minimal in order to capture only the most essential ingredients of the phenomenon. Considerable refinement is possible in a similar spirit, such as more complex client architecture, competing receptor types [36], and kinetic control by manipulation of the free energy profiles.

Raw data relating to this work can be found at [37].

A. T. R. C. is grateful for financial support from the Engineering and Physical Sciences Research Council (U.K.) through the Soft Matter and Functional Interfaces Centre for Doctoral Training (SOFI-CDT), Grant No. EP/L015536/1.

*halim.kusumaatmaja@durham.ac.uk
†m.a.miller@durham.ac.uk

[1] F. J. Martinez-Veracoechea and D. Frenkel, Proc. Natl. Acad. Sci. U.S.A. **108**, 10963 (2011).
[2] C. B. Carlson, P. Mowery, R. M. Owen, E. C. Dykhuizen, and L. L. Kiessling, ACS Chem. Biol. **2**, 119 (2007).
[3] Z. Zhang, M. M. Ali, M. A. Eckert, D.-K. Kang, Y. Y. Chen, L. S. Sender, D. A. Fruman, and W. Zhao, Biomaterials **34**, 9728 (2013).
[4] J. Huskens, A. Mulder, T. Auletta, C. A. Nijhuis, M. J. W. Ludden, and D. N. Reinhoudt, J. Am. Chem. Soc. **126**, 6784 (2004).
[5] C. T. Varner, T. Rosen, J. T. Martin, and R. S. Kane, Biomacromolecules **16**, 43 (2015).
[6] G. V. Dubacheva, T. Curk, R. Auzély-Velty, D. Frenkel, and R. P. Richter, Proc. Natl. Acad. Sci. U.S.A. **112**, 5579 (2015).
[7] M. Mammen, S.-K. Choi, and G. M. Whitesides, Angew. Chem., Int. Ed. Engl. **37**, 2754 (1998).
[8] S. Jain, J. R. Wheeler, R. W. Walters, A. Agrawal, A. Barsic, and R. Parker, Cell **164**, 487 (2016).
[9] S. F. Banani, H. O. Lee, A. A. Hyman, and M. K. Rosen, Nat. Rev. Mol. Cell Biol. **18**, 285 (2017).
[10] S. Kroschwald and S. Alberti, Cell **168**, 947 (2017).
[11] Y. Shin and C. P. Brangwynne, Science **357**, eaaf4382 (2017).
[12] S. F. Banani, A. M. Rice, W. B. Peeples, Y. Lin, S. Jain, R. Parker, and M. K. Rosen, Cell **166**, 651 (2016).
[13] K. Fong, Y. Li, W. Wang, W. Ma, K. Li, R. Z. Qi, D. Liu, Z. Songyang, and J. Chen, J. Cell Biol. **203**, 149 (2013).
[14] T. S. Harmon, A. S. Holehouse, M. K. Rosen, and R. V. Pappu, eLife **6**, e30294 (2017).
[15] J. A. Ditlev, L. B. Case, and M. K. Rosen, J. Mol. Biol. **430**, 4666 (2018).
[16] N. Kedersha, M. R. Cho, W. Li, P. W. Yacono, S. Chen, N. Gilks, D. E. Golan, and P. Anderson, J. Cell Biol. **151**, 1257 (2000).
[17] S. Boeynaems *et al.*, Proc. Natl. Acad. Sci. U.S.A. **116**, 7889 (2019).
[18] M. Dundr, M. D. Hebert, T. S. Karpova, D. Stanek, H. Xu, K. B. Shpargel, U. T. Meier, K. M. Neugebauer, A. G. Matera, and T. Misteli, J. Cell Biol. **164**, 831 (2004).
[19] Y. Jo and Y. Jung, Chem. Sci. **11**, 1269 (2020).
[20] See Supplemental Material at http://link.aps.org/supplemental/10.1103/PhysRevLett.126.028002 for further details on the simulation method, which includes Refs. [21–24], as well as additional results on the directed and isotropic binding cases.
[21] D. Frenkel and B. Smit, *Understanding Molecular Simulation* (Academic Press, New York, 2001), p. 29.
[22] S. Kroschwald, S. Maharana, D. Mateju, L. Malinovska, E. Nüske, I. Poser, D. Richter, and S. Alberti, eLife **4**, e06807 (2015).
[23] W. Xing, D. Muhlrad, R. Parker, and M. K. Rosen, eLife **9**, e56525 (2020).
[24] K. K. Nakashima, M. A. Vibhute, and E. Spruijt, Front. Mol. Biosci. **6**, 21 (2019).
[25] P. Li *et al.*, Nature (London) **483**, 336 (2012).
[26] Y. Lin, D. S. Protter, M. K. Rosen, and R. Parker, Molec. Cell **60**, 208 (2015).
[27] D. S. Protter, B. S. Rao, B. Van Treeck, Y. Lin, L. Mizoue, M. K. Rosen, and R. Parker, Cell Rep. **22**, 1401 (2018).
[28] G. V. Dubacheva, T. Curk, B. M. Mognetti, R. Auzély-Velty, D. Frenkel, and R. P. Richter, J. Am. Chem. Soc. **136**, 1722 (2014).
[29] P. Varilly, S. Angioletti-Uberti, B. M. Mognetti, and D. Frenkel, J. Chem. Phys. **137**, 094108 (2012).

[30] J. R. Wheeler, T. Matheny, S. Jain, R. Abrisch, and R. Parker, eLife **5**, e18413 (2016).
[31] N. Kedersha, G. Stoecklin, M. Ayodele, P. Yacono, J. Lykke-Andersen, M. J. Fritzler, D. Scheuner, R. J. Kaufman, D. E. Golan, and P. Anderson, J. Cell Biol. **169**, 871 (2005).
[32] S. Kroschwald, S. Maharana, D. Mateju, L. Malinovska, E. Nüske, I. Poser, D. Richter, and S. Alberti, eLife **4**, e06807 (2015).
[33] A. S. Hoffman, Adv. Drug Delivery Rev. **64**, 18 (2012).
[34] I. Y. Jung, J. S. Kim, B. R. Choi, K. Lee, and H. Lee, Adv. Healthcare Mater. **6**, 1601475 (2017).
[35] C. Stoffelen and J. Huskens, Nanoscale **7**, 7915 (2015).
[36] S. Angioletti-Uberti, Phys. Rev. Lett. **118**, 068001 (2017).
[37] https://dx.doi.org/10.15128/r1rn301144c.